Published in: Journal of Nuclear Materials 456 (2015) 106–110

Erosion at the inner wall of JET during the discharge campaign 2011-2012 in comparison with previous campaigns

S. Krat[1], Yu. Gasparyan[1], A. Pisarev[1], I. Bykov[2], M. Mayer[3†], G. de Saint Aubin[3], M. Balden[3], C.P. Lungu[4], A. Widdowson[5], JET-EFDA contributors[*]

JET-EFDA, Culham Science Centre, Abingdon, OX14 3DB, UK

[1]National Research Nuclear University "MEPhI", Moscow Kashirskoe shosse 31, 115409, Russia

[2]Fusion Plasma Physics, Royal Institute of Technology (KTH), Teknikringen 31, Stockholm 10044, Sweden

[3]Max-Planck-Institut für Plasmaphysik, Boltzmannstr. 2, 85748 Garching, Germany

[4]NILPRP, Association EURATOM-MEdC, Bucharest, Romania

[5]Culham Science Centre, EURATOM/UKAEA – Fusion Association, Abingdon, Oxfordshire OX14 3DB, UK

Abstract

The erosion of Be and W marker layers was investigated using long-term samples during the first ITER-like wall discharge campaign 2011-2012. The markers were mounted in Be coated Inconel tiles between the inner wall guard limiters (IWGL). They were analyzed using Rutherford backscattering (RBS) before and after exposure. All samples showed strong erosion. The results were compared to the data for Be and W erosion rates for the 2005-2009 and the 2001-2004 campaigns, respectively, when JET was operated with a carbon wall. In 2005-2009 Be and C samples were used, and W samples were used in 2001-2004. The mean W erosion rates and the toroidal and poloidal distributions of the W erosion were the same for the 2001-2004 and the 2011-2012 campaigns. The mean erosion rate of Be during the 2011-2012 campaign was smaller by a factor of about two compared to the 2005-2009 campaign and showed a different poloidal distribution. The mean erosion rate of the inner JET ITER-like wall was about 4-5 times smaller than the mean erosion rate of the carbon wall.

[*]See the appendix of F.Romanelli *et al.*, Proc 24th IAEA Fusion Energy Conference 2012, San Diego, USA

[†]Corresponding author. E-mail: matej.mayer@ipp.mpg.de; Tel.: ++49 89 32991639; Fax.: ++49 89 32992279

Introduction.

Erosion and redeposition of plasma facing materials are important processes which influence component lifetime and tritium inventory in thermonuclear installations. During the carbon-dominated operational phases of JET, i.e. prior to the installation of the JET ITER-like wall in 2010, thick redeposited layers were observed on all inner divertor tiles, in remote areas of the inner and outer divertor, and on parts of outer divertor tile 6 (the outermost horizontal tile at the divertor bottom) [1-3]. The layers consisted mainly of carbon, with some beryllium and metals (Ni, Fe, Cr) from the Inconel wall [4]. These layers contained large amounts of deuterium due to codeposition [5-6].

The inner wall of JET consists of inner wall guard limiters (IWGLs) with recessed areas between them. These recessed areas are the inner wall cladding and showed substantial net material erosion during the carbon operational phases [7-10]. They could be identified as an important net carbon source, from where large amounts of carbon were eroded and transported to the divertor, where the carbon was redeposited.

Before the start of the experimental campaign of 2011-2012 [11], the wall and the divertor of JET were changed and the ITER-like wall (ILW) was installed [12]. Bulk beryllium on Inconel carriers was used for the inner and outer limiters, while W coated carbon fibre composite (CFC) was used for some IWGL tiles with recessed centre sections in the areas of increased heat flux. Be coated Inconel tiles were used at a selection of IWGLs with recessed central part and as the inner wall cladding between the IWGLs. Tungsten coated CFC tiles with no active cooling were used in the divertor with a single toroidally continuous belt of bulk tungsten at the outer strike point.

These modifications are likely to affect the erosion-deposition patterns in JET. Some of the changes have already been identified [13]. They include an increased Be erosion rate for the mid-plane IWGLs, decreased overall deposition in the divertor, with migration of material to remote areas at least one order of magnitude smaller than during the carbon phase.

The changed divertor deposition pattern with the ITER-like wall raises the question, if the net erosion source pattern has been modified as well. In this paper, experimental results from long-term samples (LTS) installed during the 2011-1012 operational campaign at the inner wall cladding, i.e. at the recessed parts of the JET inner wall between IWGLs, are discussed and compared to the results obtained with LTS during the 2001-2004 and 2005-2009 campaigns with carbon walls [10].

Experimental

Nine LTS were exposed during the 2011-2012 discharge campaign [14]. The samples were made of Inconel and mounted as sachet inserts in beryllium coated Inconel tiles between IWGLs. All Inconel surfaces including the LTS surfaces were artificially roughened by sand-blasting, scanning electron microscopy images before the exposure are shown in Fig. 1. Figure 2 shows the positions of the LTS: four samples were mounted in octant 4 at different poloidal

locations (tiles 2, 5, 8 and 11), five samples were mounted close to the inner midplane in the 8th tiles in different octants (octants 1, 2, 5, 6 and 8). Each sample number contains information about the toroidal and poloidal location, i.e. sample "208" was exposed in octant 2, tile 8. Tile 8 is close to the inner midplane, decreasing tile numbers are towards the top of the machine, increasing tile numbers are towards the divertor.

One half of the LTS surface was coated with tungsten using physical vapor deposition, resulting in about 42 nm thick tungsten layers. The other half was coated with Be layers of approximately 2.5 μm thickness.

The samples were analyzed using ion beam analysis before and after exposure. Rutherford backscattering (RBS) using 1.6 MeV protons was used for measurement of the layer thicknesses. The detector was mounted at a scattering angle of 165°. The SIMNRA code [15] with SRIM 2013 stopping power was used for quantitative evaluation of the RBS spectra. The non-Rutherford scattering cross-sections from beryllium as well as the $^{9}Be(p,d)^{8}Be$ reaction cross-section were determined for the scattering angle of 165° in the energy range from 1.1 to 2.0 MeV and 1.25 to 2.0 MeV respectively using a bulk beryllium sample [16]. Non-Rutherford scattering cross-sections from [17] were used for oxygen. For W marker layers, integral values of the W RBS signal were used for fitting due to a very high sensitivity of the modeled peak's position on the detector's calibration parameters. This sensitivity can lead to discrepancies between the positions of modeled and experimentally observed peaks, making fitting their shapes more inaccurate.

Net erosion rates were calculated from the amounts of the eroded material for all samples, using total successful (I_p>0.7 MA) discharge times obtained from JET discharge statistics (table 1). Total amounts of eroded materials were calculated assuming 7.2 m^2 to be the surface area of the Be-coated recessed part of the inner wall between the inner wall guard limiters, and 4.0 m^2 be the surface area of the W-coated recessed part of the inner wall between the inner wall guard limiters.

Results and discussion.

The results have been compared to the W and Be erosion data from the 2001-2004 and 2005-2009 discharge campaigns respectively [10] (table 2).

The poloidal and toroidal distributions of the erosion rates of Be and W are shown in figure 3. RBS spectra of typical Be and W samples before and after the exposure are shown in figure 4. In the RBS spectra of all samples, rounded high-energy edges of the Inconel substrate are observed. These rounded edges are observed also on Inconel samples without marker layers and are either due to the roughened surfaces, or due to increased carbon or oxygen concentrations in the near-surface layers. This spectral feature is difficult to model. Nevertheless, W layer thicknesses still can be extracted precisely from the total number of counts in the W peak, while Be layer thicknesses can be derived from the shift of the Inconel high-energy edge and the width of the beryllium peak. The error margins for W are taken from the statistical error of the number of counts in the W peak and are smaller than the size of the dots. The error margins for Be are taken from the uncertainty in the determination of the position of the low-

energy edge of the Be signal together with the uncertainty of the position of the Inconel high-energy edge.

The net W erosion is almost homogeneous in poloidal and toroidal directions both for the 2001-2004 and 2011-2012 discharge campaigns. The net erosion rates are almost the same for both campaigns. The average net erosion rate for the area near the midplane (8^{th} tile counting from the top, see fig. 2) was $9.2 \cdot 10^{11}$ atoms/cm^2·s for the 2011-2012 campaign and $9.6 \cdot 10^{11}$ atoms/cm^2·s for the 2001-2004 campaign. The average net erosion rate for the recessed part of the inner wall taking toroidal and poloidal variations into account was $9.2 \cdot 10^{11}$ atoms/cm^2·s for the 2011-2012 campaign. The total amount of W eroded from the W-coated areas of the recessed parts of the inner wall during the whole campaign was 0.7 g. For a hypothetical full W inner wall recessed area, the total net erosion would have been about 2 g. The average net erosion rate for the 2001-2004 campaign was $8.4 \cdot 10^{11}$ atoms/cm^2·s with the total net erosion of 1.8 g for the hypothetical full W inner wall.

An increase in roughness can be observed in the RBS spectra (Fig. 4) after the exposure compared to the spectra of the same samples before exposure. The typical roughness of the Be layers was close to $4 \cdot 10^{18}$ atoms/cm^2, or roughly 300 nm before exposure and increased to $14 \cdot 10^{18}$ atoms/cm^2, or roughly 1 μm after exposure. Small signals of Ni, Cr, Fe (Inconel component materials) could be detected in the beryllium top layer both before and after the exposure. Their total average concentration before the exposure was about 0.3%, and varied from 0.4% to 1% after exposure. The oxygen concentration also increased noticeably after the exposure. Due to exposure of the samples to air after retrieval from the vessel the oxygen is hard to interpret and may be due to oxidation of the rough beryllium surface in atmosphere. Small amounts of W, about $1 \cdot 10^{15}$ atoms/cm^2, can be observed on the surface of the Be-coated samples after the exposure. The Ni, Cr, Fe and W signals are indications of (small) redeposition of Inconel components and tungsten originating from erosion processes at different areas of the machine.

Toroidal net Be erosion distributions are similar for the 2005-2009 and 2011-2012 experimental campaigns, with small maxima in the 1^{st}, 4^{th}, and 8^{th} octants. The maxima in the 4^{th} and 8^{th} octants could possibly be explained by the positions of neutral beam injectors located in these octants. Because of the injectors, either the fluxes of neutral particles striking the inner wall in those octants or the neutral particle energies might be higher than in other octants, leading to the observed slightly higher erosion rates. It has been already observed at ASDEX Upgrade, that increased neutral gas fluxes (for example due to recycling at the ICRF antennas) can cause increased erosion at the wall [18]. The poloidal distributions differ between the campaigns. For the 2005-2009 campaign, in which carbon protection tiles were used for the inner wall, the net Be erosion was almost homogeneous. The net Be erosion in the 2011-2012 campaign with the ITER-like Be inner wall shows a maximum near the midplane (8^{th} tile), with lower net erosion both in upward and downward directions. The net erosion rates were lower during the 2011-2012 campaign than during the 2005-2009 campaign by a factor of nearly 2. The average erosion rate for the area near the midplane (8^{th} tile) was $1.2 \cdot 10^{14}$ atoms/cm^2·s for the 2005-2009 campaign and $0.79 \cdot 10^{14}$ atoms/cm^2·s for the 2011-2012 campaign. The average erosion rate for the whole inner wall including the poloidal distribution was $1.2 \cdot 10^{14}$ atoms/cm^2·s for the 2005-2009 campaign (resulting in a total erosion of about 60 g for a hypothetical full beryllium wall during

that campaign), and $0.55 \cdot 10^{14}$ atoms/cm^2·s for the 2011-2012 campaign, leading to a total erosion of about 3.8 g for the ITER-like wall configuration and a hypothetical erosion for a full beryllium wall of about 5.5 g.

The measured net erosion is the sum of gross erosion, caused by sputtering and evaporation, and redeposition. The lower erosion rates observed for Be during the 2011-2012 campaign in comparison to the measured Be erosion observed during the carbon phase 2005-2009 can thus be caused by either decreased gross erosion due to smaller (or lower energetic) neutral particle fluxes, produced by charge exchange neutrals, to the inner wall, or by increased redepositon of Be eroded from the ITER-like inner wall back onto the samples, which wasn't present during the carbon phase. IWGLs could be one source of the redeposited particles; an increase of gross erosion rate in comparison to the carbon phase was observed on the IWGLs[19]. The similarities of W erosion rates in the 2001-2004 and 2011-2012 campaigns makes the difference in plasma parameters causing decreased gross erosion a less likely explanation for the change in Be erosion. Additionally, an increased concentration of Ni, Cr and Fe can be observed in the surface layers of the Be samples, which indicates redeposition. This is supported by a significant increase in Be layer roughness. W presence on the surface of Be samples also indicates that some redeposition takes place.

The carbon erosion rate of $2.4 \cdot 10^{14}$ atoms/cm^2·s during the 2005-2009 campaign [10] was 2 times higher than the beryllium erosion rate during the same campaign. This was despite the possibility of carbon redeposition from the inner wall onto the carbon samples. Carbon and beryllium sputtering yields are close to each other except for low energies of incident particles (<10 eV) [20], where the carbon erosion yield is far higher because of the chemical erosion mechanisms. Higher C erosion rates indicate a large amount of low energy neutral particles. This is in good agreement with previously published results [10]. The erosion rate of the ITER-like wall is about 4-5 times lower than the carbon wall erosion rate due to the absence of chemical erosion

The applied method determines the integral net erosion for the whole campaign and does not allow to distinguish between different discharges or discharge phases. To determine the effect of limiter and divertor phases on the erosion, modeling is required.

Conclusions

The erosion of Be and W marker layers was investigated using LTS exposed during the discharge period 2011-2012 and was compared with the Be and W erosion data from the 2005-2009 and 2001-2004 discharge periods, respectively. The marker layers were analyzed using Rutherford backscattering before and after exposure.

The average erosion rate of W markers during the discharge campaign 2011-2012 ($9.2 \cdot 10^{11}$ atoms/cm^2·s) was very close to the one for the discharge campaign 2001-2004 ($8.4 \cdot 10^{11}$ atoms/cm^2·s). In both campaigns both toroidal and poloidal erosion distributions were mostly homogeneous.

The toroidal erosion distribution of Be was similar for both 2005-2009 and 2011-2012 campaigns. The erosion distribution had small maxima in the 1st, 4th and 8th octants. The carbon net erosion rate distribution during the 2005-2009 campaign had a similar shape except for the first octant, with small maxima at the 4th and 8th octants.

The poloidal distribution had a maximum near the midplane (8th tile) and a sharp decrease in erosion towards the bottom (11th tile) during the 2011-2012 campaign and was mostly homogeneous (with a maximum difference of 15% in erosion between tiles) during the 2005-2009 campaign.

The average net erosion rate of the Be markers during the discharge campaign 2011-2012 ($0.55 \cdot 10^{14}$ atoms/cm^2·s) was about 50% of that for the discharge campaign 2005-2009 ($1.2 \cdot 10^{14}$ atoms/cm^2·s). This means that the net erosion rate for the ITER-like inner wall of JET was about 1/5th - 1/4th of that for the carbon-coated inner wall. Be redeposition from the limiters or from the recessed inner wall tiles is a possible explanation of this decrease, compared to the net erosion rate of Be during the 2005-2009 campaign. Chemical erosion of C by low energy particles is the most probable explanation for the comparatively lower Be net erosion rate during the 2005-2009 campaign.

References

[1] J.P. Coad, N. Bekris, J.D. Elder, S.K. Erents, D.E. Hole, K.D. Lawson, G.F. Matthews, R.D. Penzhorn, P.C. Stangeby, Erosion/deposition issues at JET, Journal of Nuclear Materials, 290–293 (2001) 224-230.

[2] J.P. Coad, P. Andrew, D.E. Hole, S. Lehto, J. Likonen, G.F. Matthews, M. Rubel, Erosion/deposition in JET during the period 1999–2001, Journal of Nuclear Materials, 313–316 (2003) 419-423.

[3] J.P. Coad, P. Andrew, S.K. Erents, D.E. Hole, J. Likonen, M. Mayer, R. Pitts, M. Rubel, J.D. Strachan, E. Vainonen-Ahlgren, A. Widdowson, Erosion and deposition in the JET MkII-SRP divertor, Journal of Nuclear Materials, 363–365 (2007) 287-293.

[4] J. Likonen, E. Vainonen-Ahlgren, L. Khriachtchev, J.P. Coad, M. Rubel, T. Renvall, K. Arstila, D.E. Hole, Structural investigation of re-deposited layers in JET, Journal of Nuclear Materials, 377 (2008) 486-491.

[5] J. Likonen, J.P. Coad, D.E. Hole, S. Koivuranta, T. Renvall, M. Rubel, E. Vainonen-Ahlgren, A. Widdowson, Post-mortem measurements of fuel retention at JET with MKII-SRP divertor, Journal of Nuclear Materials, 390–391 (2009) 631-634.

[6] S. Koivuranta, J. Likonen, A. Hakola, J.P. Coad, A. Widdowson, D.E. Hole, M. Rubel, Post-mortem measurements of fuel retention at JET in 2007–2009 experimental campaign, Journal of Nuclear Materials, 438, Supplement (2013) S735-S737.

[7] M. Mayer, R. Behrisch, P. Andrew, J.P. Coad, A.T. Peacock, Transport and Redeposition of Eroded Material in JET, Physica Scripta T81 (1999) 13-18.

[8] M. Mayer, R. Behrisch, P. Andrew, A.T. Peacock, Erosion at the vessel walls of JET, Journal of Nuclear Materials, 241–243 (1997) 469-475.

[9] M. Mayer, R. Behrisch, K. Plamann, P. Andrew, J.P. Coad, A.T. Peacock, Wall erosion and material transport to the Mark I carbon divertor of JET, Journal of Nuclear Materials, 266–269 (1999) 604-610.

[10] M. Mayer, S. Krat, J.P. Coad, A. Hakola, J. Likonen, S. Lindig, A. Widdowson, Erosion at the inner wall of JET during the discharge campaigns 2001–2009, Journal of Nuclear Materials, 438, Supplement (2013) S780-S783.

[11] G.F. Matthews, Plasma operation with an all metal first-wall: Comparison of an ITER-like wall with a carbon wall in JET, Journal of Nuclear Materials, 438, Supplement (2013) S2-S10.

[12] G.F. Matthews, M. Beurskens, S. Brezinsek, M. Groth, E. Joffrin, A. Loving, M. Kear, M.L. Mayoral, R. Neu, P. Prior, V. Riccardo, F. Rimini, M. Rubel, G. Sips, E. Villedieu, P.d. Vries, M.L. Watkins, E.-J. contributors, JET ITER-like wall—overview and experimental programme, Physica Scripta, T145 (2011) 014001.

[13] A. Widdowson, E. Alves, C.F. Ayres, A. Baron-Wiechec, S. Brezinsek, N. Catarino, J.P. Coad, K. Heinola, J. Likonen, G.F. Matthews, M. Mayer, M. Rubel, Material migration patterns and overview of first surface analysis of the JET ITER-like wall, Physica Scripta, T159 (2014).

[14] M. Rubel, J.P. Coad, A. Widdowson, G.F. Matthews, H.G. Esser, T. Hirai, J. Likonen, J. Linke, C.P. Lungu, M. Mayer, L. Pedrick, C. Ruset, Overview of erosion–deposition diagnostic tools for the ITER-Like Wall in the JET tokamak, Journal of Nuclear Materials, 438, Supplement (2013) S1204-S1207.

[15] M. Mayer, SIMNRA User's Guide, in, Max-Planck-Institut für Plasmaphysik, Germany, Garching, Germany, 1997.

[16] M. Mayer, B. Wielunska, unpublished results.

[17] A.F. Gurbich, Evaluation of non-Rutherford proton elastic scattering cross section for oxygen, Nuclear Instruments and Methods in Physics Research Section B: Beam Interactions with Materials and Atoms, 129 (1997) 311-316.

[18] A. Tabasso, H. Maier, J. Roth, K. Krieger, Studies of tungsten erosion at the inner and outer main chamber wall of the ASDEX Upgrade tokamak, Journal of Nuclear Materials, 290-293 (2001) 326-330.

[19] K. Heinola, C.F. Ayres, A. Baron-Wiechec, J.P. Coad, J. Likonen, G.F. Matthews, A. Widdowson, J.-E. Contributors, Tile profiling analysis of samples from the JET ITER-like wall and carbon wall, Physica Scripta, T159 (2014) 014013.

[20] W. Eckstein, Sputtering yields in: R. Behrisch, W. Eckstein (Eds.) Sputtering by Particle Bombardment, Topics in Applied Physics, 2007, pp. 33-187.

Figure 1: Scanning electron microscopy images of Be (on the left) and W (on the right) layers on the LTS surfaces before exposure, 500x magnification.

Figure 2: Positions of long-term samples (LTS) in the ITER-like inner wall of JET during the discharge campaign 2011-2012. The numbers at the bottom indicate the octant number, where each octant is a 45° large sector of the torus. Tiles are numbered from top to bottom.

Figure 3: Poloidal and toroidal distributions of the erosion rates of W and Be during the 2011-2012 discharge campaign in comparison to the data for the 2005-2009 and 2001-2004 campaigns, respectively.

Figure 4: Typical RBS spectra before and after exposure for Be (on the left) and W (on the right) coated LTS. The Be spectrum includes a magnified area marked by the black rectangle on the spectrum.

Table 1: JET discharge statistics for the 2001-2004, 2005-2009 and 2011-2012 discharge campaigns.

Table 2: Overview of LTS materials, average net total LTS erosion, and net erosion rates for the 2001-2004, 2005-2009 and 2011-2012 discharge campaigns.

Discharge campaign	Number of discharges	Number of successful discharges (I_p>0.7 MA)	Total discharge time (I_p>0.7 MA), 10^4 s	Divertor phase discharge time, 10^4 s	Limiter phase discharge time, 10^4 s
2001-2004	9088	6760	17.0	11.6	5.4
2005-2009	15931	12042	30.6	23.6	7.0
2011-2012	3812	2819	6.41	4.51	1.9

Table 1

Campaign	Sample material	Average total erosion, 10^{15} atoms/cm^2	Average erosion rate, atoms/cm^2·sec
2001-2004	W	140	$8.4 \cdot 10^{11}$
2005-2009	Be	36000	$1.2 \cdot 10^{14}$
	C	74000	$2.4 \cdot 10^{14}$
2011-2012	W	60	$9.2 \cdot 10^{11}$
	Be	3500	$0.55 \cdot 10^{14}$

Table 2

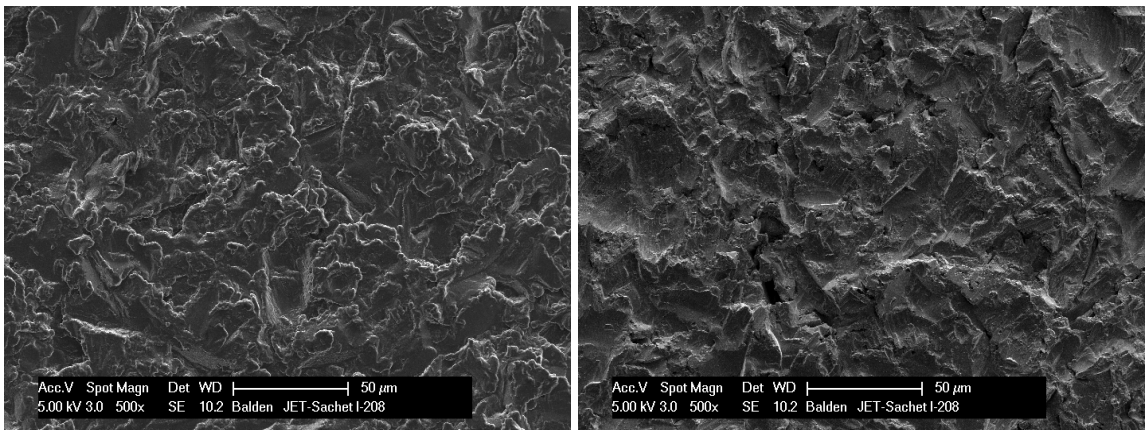
Acc.V Spot Magn Det WD 50 µm
5.00 kV 3.0 500x SE 10.2 Balden JET-Sachet I-208
Acc.V Spot Magn Det WD 50 µm
5.00 kV 3.0 500x SE 10.2 Balden JET-Sachet I-208

Figure 1

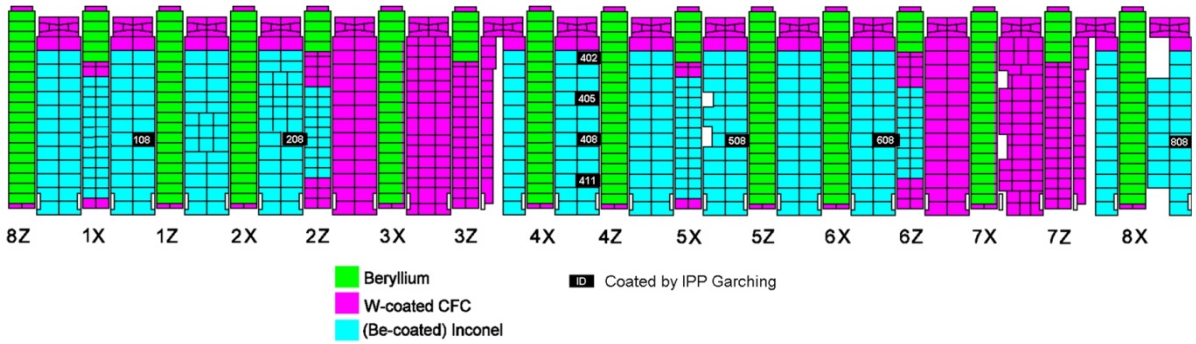
402
405
408
411
108
208
508
608
808
8Z
1X
1Z
2X
2Z
3X
3Z
4X
4Z
5X
5Z
6X
6Z
7X
7Z
8X
Beryllium
W-coated CFC
(Be-coated) Inconel
ID
Coated by IPP Garching

Figure 2

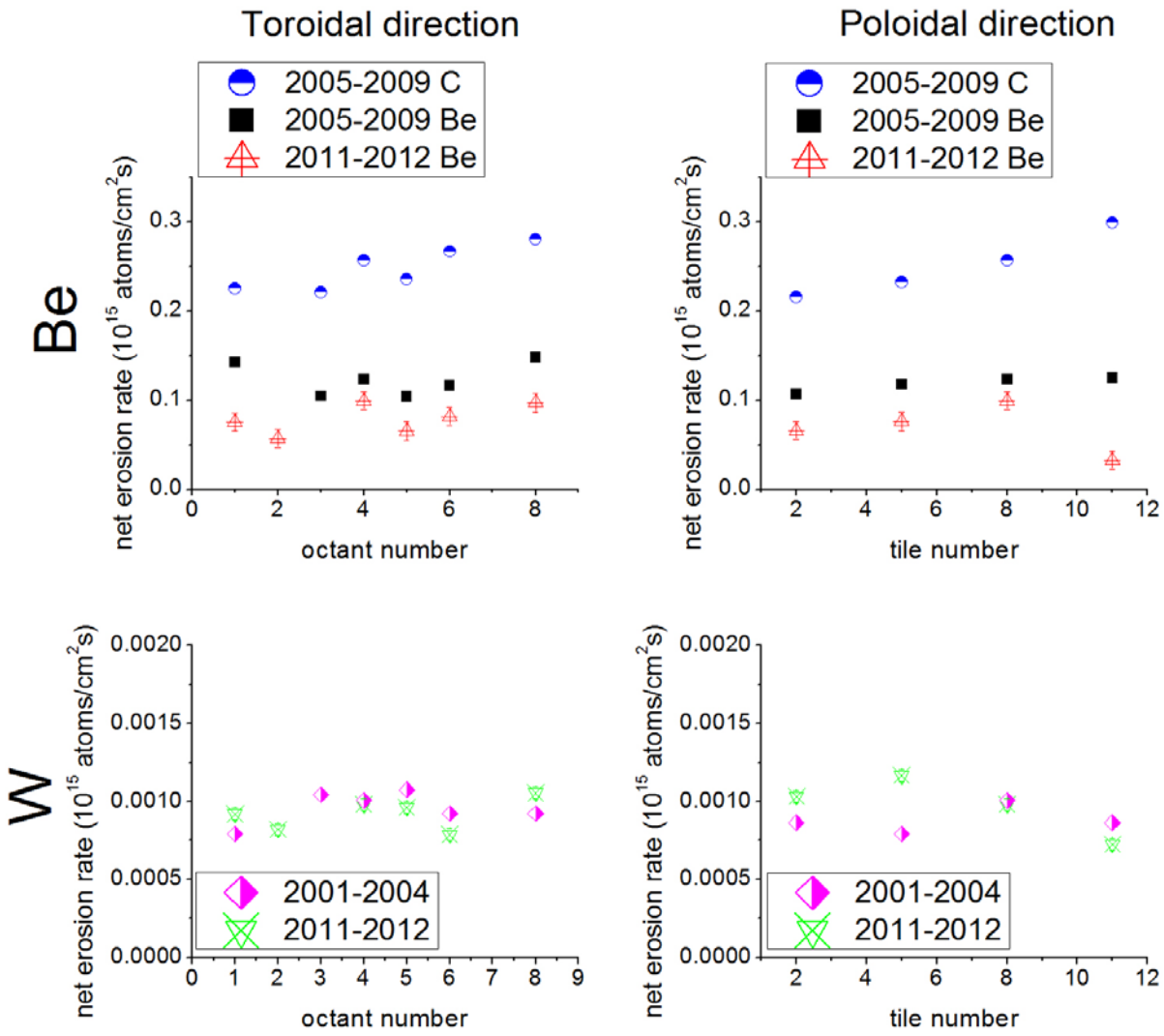
Toroidal direction
Poloidal direction
Be
W
2005-2009 C
2005-2009 Be
2011-2012 Be
2001-2004
2011-2012
net erosion rate (10^{15} atoms/cm^{2}s)
octant number
tile number

Figure 3

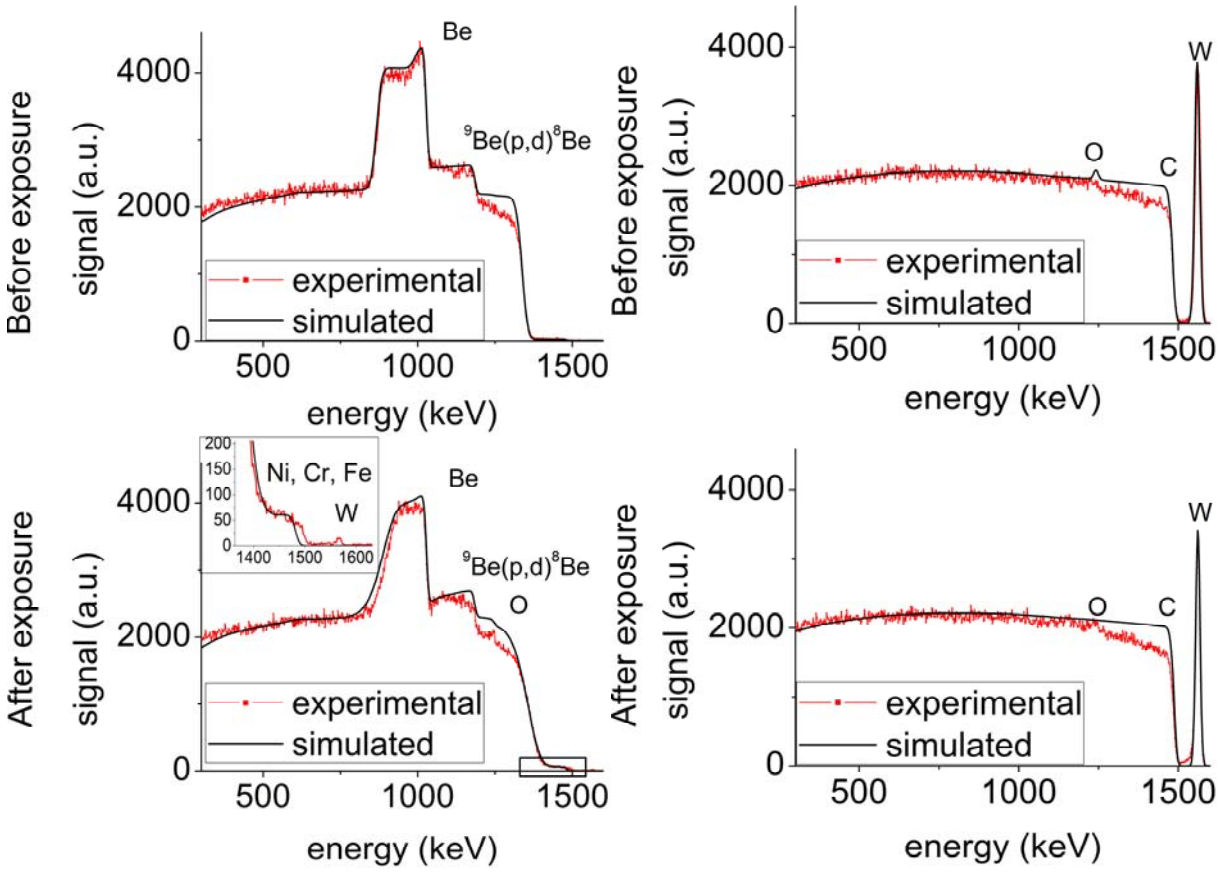
Before exposure
signal (a.u.)
4000
2000
0
500
1000
1500
energy (keV)
Be
^{9}Be(p,d)^{8}Be
experimental
simulated
O
C
W
After exposure
Ni, Cr, Fe
200
150
100
50
0
1400
1500
1600

Figure 4